京都大学防災研究所年報 第 63 号 B
DPRI Annuals, No. 63 B, 2020

Risk of Rainfall-Triggered Landslide Disasters Under Climate Change by Applying Critical Line Method to NHRCM05

Ying-Hsin WU, Eiichi NAKAKITA and Masaru KUNITOMO(1)

(1) Tohoku Regional Development Bureau, Ministry of Land, Infrastructure, Transport and Tourism, Japan

Synopsis

We present a study on the future changes of landslide risk in Japan by applying the critical line method to the 5-km regional climate model of NHRCM05. From the six datasets of NHRCM05, we extracted effective rainfall events from the parameter of surface precipitation without any interpolation. In all extracted rainfall events, the critical line method was applied to obtain the frequency of landslide occurrence at each 1 by 1-km grid in the whole Japan. We exhibit the future changes of nationwide landslide risk distribution, monthly occurrence frequency in each geographical region, and occurrence trend in each prefecture. Additionally, from a different perspective, we reveal the relation between landslide risk trend and the geological feature of plate tectonics. As a result, the landslide risk is higher in the early summer of July in west Japan and in the late summer of September in east Japan. Particularly, the analysis shows a significant increasing trend of landslide risk in the Hokkaido area.

Keywords: landslide risk, critical line, early-warning, climate change, NHRCM05

1. Introduction

In the last three years, Baiu fronts and typhoons brought huge amount of rainfall in several regions in west and east Japan to trigger numerous severe inundation and landslide disasters and to cause fatalities and much property damages. For the current early warning of landslide hazards, governmental authorities, i.e., Ministry of Land, Infrastructure, Transport and Tourism (abbreviated as MLIT), Japan Meteorological Agency (JMA), and prefectural governments, assess hazard occurrence by using high-resolution radar rainfall data and the famous critical line method (Osanai et al., 2010). The critical line method can practically forecast landslide occurrence by two hydrometeorological indices representing short- and long-term conditions prone to landslide hazards, i.e., hourly rainfall intensity and soil-water index (SWI), respectively. To judge hazard occurrence over a given 1-km^2 region by the two hydrometeorological indices, a critical line is specifically calibrated by applying the nonlinear regression of radial basis function network (Osanai et al., 2010) to past landslide events. With best calibration for the whole Japan, the critical line method has successfully predicted couples of landslide hazards and currently been applying for real-time landslide early warning.

Recently, extreme climate becomes more frequent worldwide to trigger considerable numbers of water-related disasters, and has raised the great attention of the public and scientific communities. Recent extreme rainfall events show some obvious changes that rainfall period was elongated with very high accumulated rainfall amount and hourly rainfall intensity which have made new records of observation in many places. Consequently, numerous devastating floods, landslides and

sediment disasters have occurred in a situation beyond people's past experience. Some research has indicated that one dominant factor to induce extreme climate is the increased average earth-surface temperature, which is termed as global warming phenomenon and brought out by the great amount of greenhouse gases emitted from industrial development in the last century. As global warming is a long-term heating of the earth's atmosphere, extreme weather would take place more often in the future, and future rainfall could be more intense in a shorter duration with a higher totally accumulated amount, which are the main factors to intensify landslides and sediment hazards. Some research has examined historical landslides associated with rainfall (Saito et al., 2014) and nationwide landslide hazard susceptibility (Kawagoe et al., 2010), but the future trend is still open for answers. So, we are motivated to know where, when and how future landslide will occur in Japan in this changing climate.

For our objective, we would like to utilize the critical line method with all critical lines obtained by courtesy of MLIT and each prefectural government. To analyze landslides which is a local slope process, it requires rainfall data in a spatial resolution finer than the order of magnitude of several tens of kilometers. So, for the representative future climate, we adopted the famous 5-km Non-Hydrostatic Regional Climate Model (often called NHRCM05), developed by Meteorological Research Institute of JMA (Murata et al, 2014; Murata et al., 2015; Sasaki et al., 2011; Sasaki et al., 2012). Additionally, landslide process is highly related to local slope's geological features determined by the tectonic activities of earth lithosphere. As is located at the joint boundaries of Eurasian, North American, and Philippine tectonic plates (Takahashi, 2016), where is an earthquake hot zone with active orogenesis, Japanese archipelago possesses diverse geologic settings. However, the current critical lines are calibrated only by hydrometeorological factors, the impact of geologic settings on landslide risk is still implicit in the application of critical line method. So, to reveal the explicit influence of tectonic setting in the near future, we further explore relations between landslide risk and changing climate in each tectonic zone of Japan, respectively.

The major merit of this research is to exhibit the future changes of landslide risk in Japan by pointing out the spatiotemporal information of high-risk situation of landslides. It is convinced that the future landslide risk obtained from this research can be a valuable reference for future disaster management and policy making of sustainable development.

2. Data and Methods

2.1 NHRCM05

The spatiotemporal resolution is 5 km in space and 30 minutes in time. The model domain consists of 527×804 grids covering Japanese archipelago. As is listed in Table 1, SPA represents the present climate, and the others (SFA_26, SFA_c1, SFA_c2, SFA_c3, and SFA_c0) for future climate. The domain boundary conditions are derived from simulations of MRI-AGCM3.2S4). The scenarios of future projections are Representative Concentration Pathway (RCP) 2.6 and 8.5, proposed in IPCC Fifth Assessment Report in 2014 for representing human activities of industrial development. Four spatial

Table 1 Brief information of NHRCM05

Dataset	Scenario	Boundary SST (Murata et al., 2014)	Simulation Period
SPA	-	Monthly observation (1979-2003)	From 1980/09/01 To 2000/08/30
SFA_26	RCP2.6	El Niño	From 2076/09/01 To 2095/08/30
SFA_c1	RCP8.5	Less warmer in East tropical Pacific	
SFA_c2	RCP8.5	Stronger El Niño	
SFA_c3	RCP8.5	Warmer in Northwest Pacific	
SFA_c0	RCP8.5	El Niño	

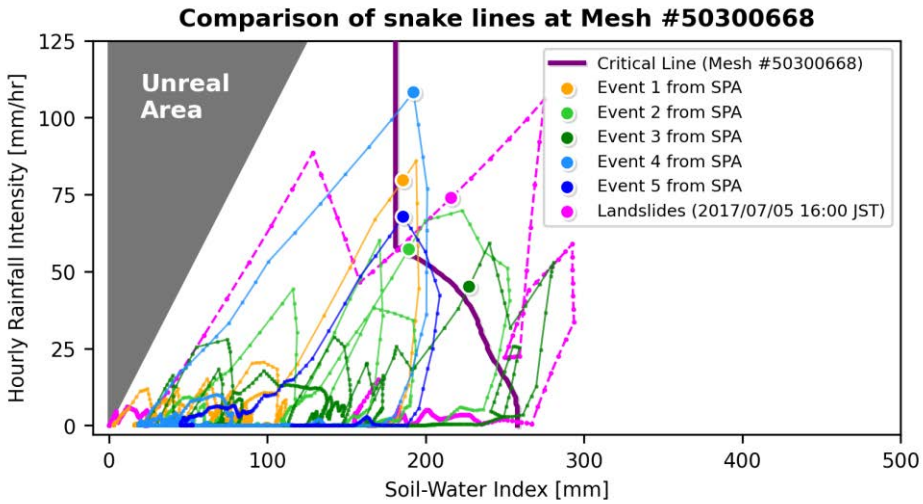

Fig. 1 Comparison of the snake lines of landslides in Asakura on 5 July 2017 16:00 (JST) and five events extracted from the present climate of NHRCM05 (SPA).

patterns of sea-surface temperature (SST) (Murata et al, 2014) were imposed as the sea surface boundary condition in the future projection simulations. The simulation period of each dataset is 20 years with a one-year time slice and a spin-up period of from July 21 to September 1.

Comparison between the present climate simulations and AMeDAS observation has verified that NHRCM05 can well reproduce the spatial distribution and seasonal changes of annual precipitation with a small bias of precipitation at few points along the coast of Japan Sea (Sasaki et al, 2011; Sasaki et al., 2012). Also, the verification of future projection of NHRCM05 displays that the increase of frequency of rainfall greater than 10 mm is at 99% confidence level, and projected cyclones approach Japanese archipelago to cause more precipitation along the Pacific coast (Sasaki et al., 2012). Although holding acceptable errors, NHRCM05 is regarded as one 5-km climate model best representing regional climate around Japan by considering the effect of El Niño-Southern Oscillation phenomenon. Our analysis only used the parameter of surface precipitation, and the direct extraction of was applied to the parameter without any interpolation method.

2.2 Extraction of Landslide Events

The resolution of each grid which a critical line applies to is 1 km^2. We processed rainfall data to extract rainfall events corresponding to high landslide risk situation at each 1 km^2 grid. As the NHRCM05 datasets are computed in the one-year time slice, we processed all data in the same manner. Firstly, the continuous rainfall series in each year from each dataset was extracted at each grid, and the continuous time series of SWI (Osanai et al., 2010) in each one-year time slice was calculated. Then, to prevent from duplicate counting of one event, we extracted all effective rainfall events (MLIT, 2005) for check. Finally, the time series of hourly rainfall and SWI were applied to judge whether the pair of the two parameters at each grid passes through the corresponding critical line of that grid. Within one effective rainfall event, only one landslide event is counted no matter how many times the critical line is crossed. The occurrence timing for each event is also extracted for the analysis. Fig. 1 shows the comparison of one real landslide event with other events extracted from SPA at the mesh of 50300668, where the longitude and latitude are 130.85E and 33.39N, respectively, in Akatanigawa area in Asakura City in Fukuoka. Obviously, the computed snake lines from datasets of NHRCM05 are very similar to the snake line of a real event obtained by radar rainfall data. Therefore, our analysis could be considered reliable.

To gently remind, the occurrence frequency hereafter denotes the total number of rainfall events corresponding to high landslide risk situation in different climate scenarios, but definitely not the one of real landslide prediction.

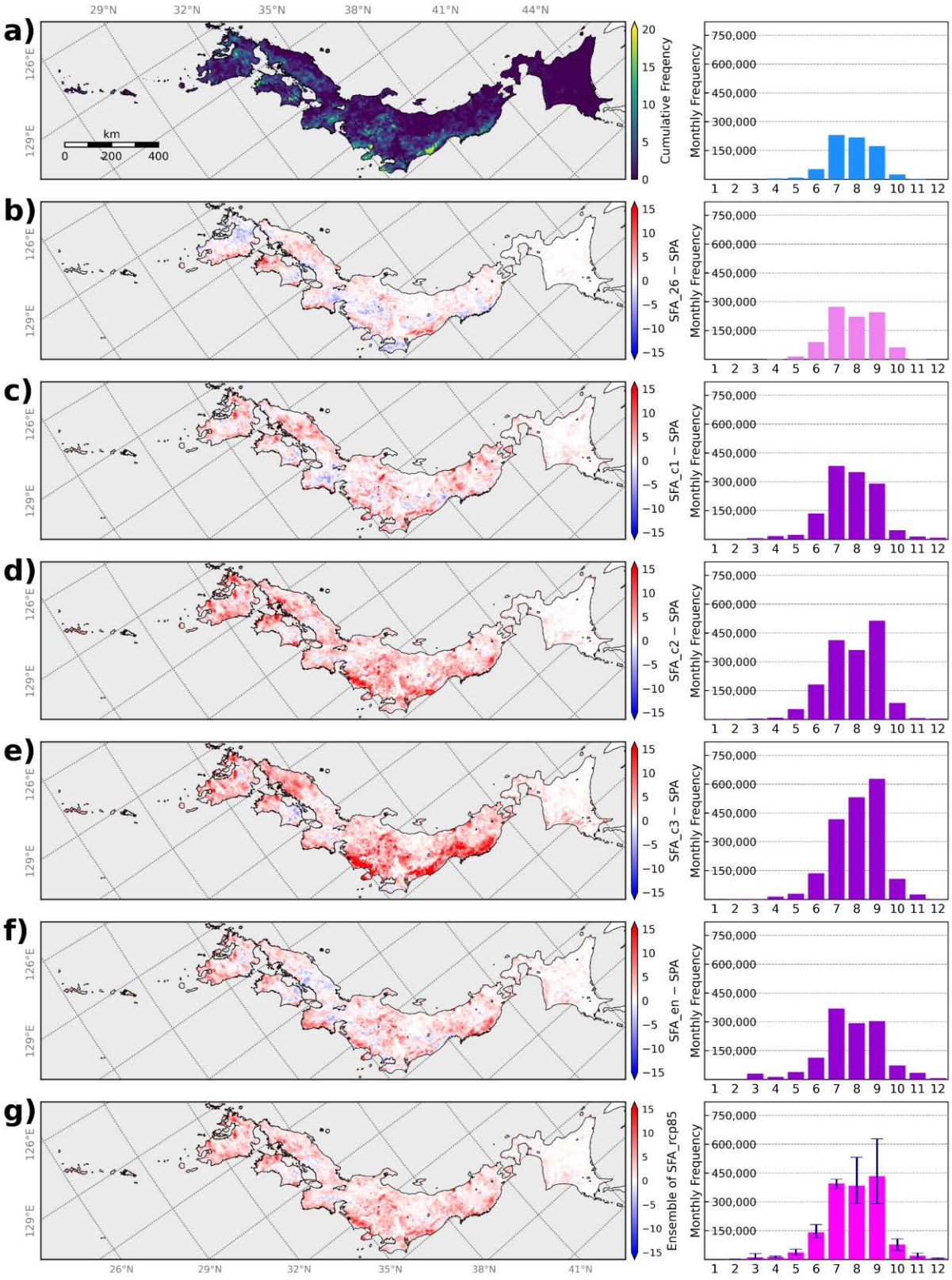

Fig. 2 Nationwide landslide risk and monthly frequency from all NHRCM05 datasets: a) frequency of present climate dataset of SPA, and the future changes of frequency of b) SFA_26, c) SFA _c1, d) SFA_c2, e) SFA_c3, and f) SFA_c0 deviated from SPA. Subfigures g) are ensemble mean of datasets from c) to f), and the error bars denote maximum and minimum frequencies. The monthly frequency denotes the accumulated frequency from each dataset in each month in 20 years.

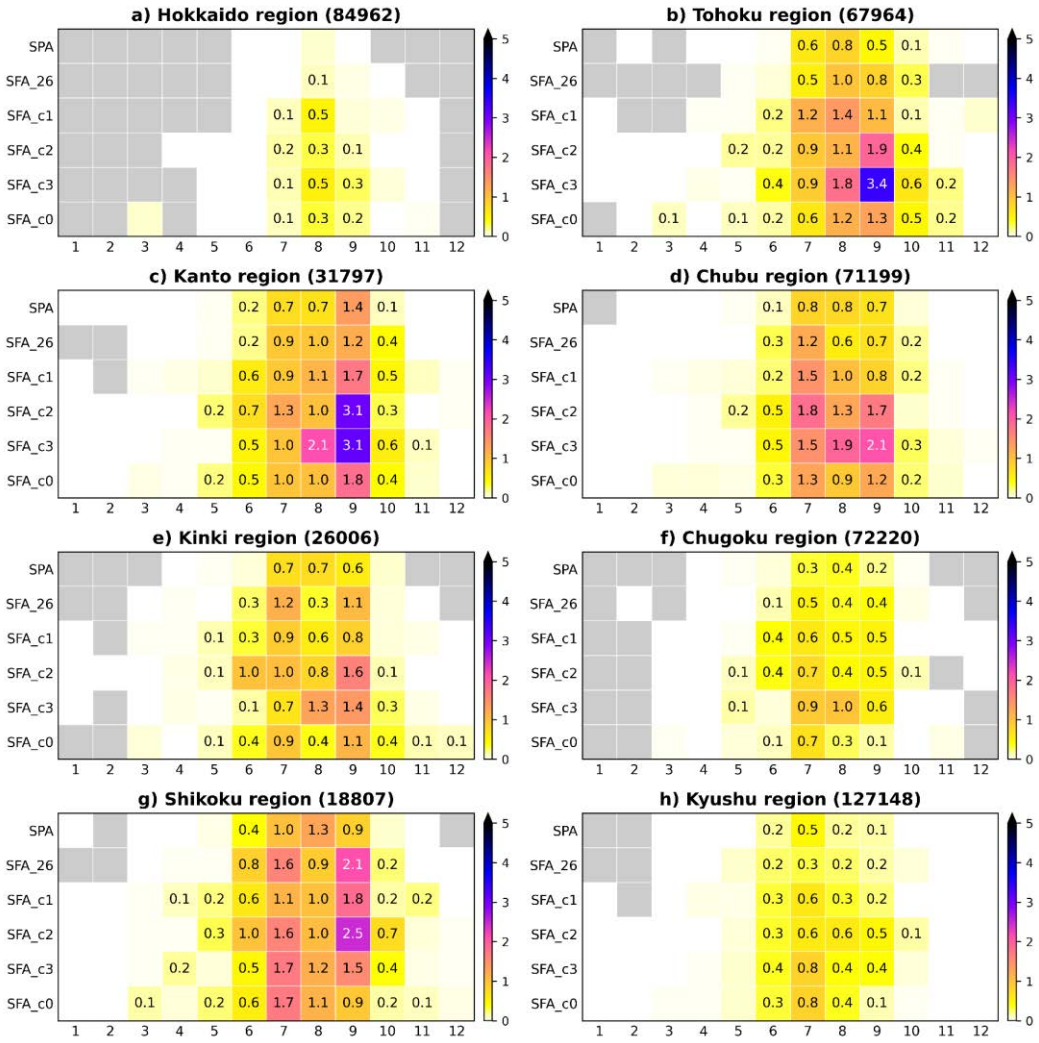

Fig. 3 Normalized monthly frequency from all NHRCM05 datasets in all geographical regions: a) Hokkaido, b) Tohoku, c) Kanto, d) Chubu, e) Kinki, f) Chugoku, g) Shikoku, and h) Kyushu regions. The total grid number in each region is denoted in brackets. The cell values and colors denote the normalized monthly frequency. Gray color denotes non-occurrence.

3. Results and Discussion

3.1 Nationwide Landslide Risk

Fig. 2 illustrates the nationwide distribution of landslide risk from the present climate dataset SPA and its future changes, and the cumulative monthly frequency from all datasets. The results clearly show landslide risk becomes higher along the coast of Pacific Ocean and in eastern Shikoku and northern Kyushu. Particularly, as is shown in Fig. 2e, along the coast of northwest Pacific Ocean, a significant increase of landslide event appears along the coast area of Aichi, Shizuoka, Ibaraki, Fukushima, Miyagi, and Iwate prefectures. Oppositely, a clear decrease of occurrence is found in east Shikoku and Chugoku regions as well as central Kii peninsula in the Kinki region. Finally, a slight increase is also revealed in east and south Hokkaido. Besides, the monthly accumulated frequency shows that the estimated occurrence becomes higher from June to October in the future.

3.2 Monthly Frequency in Geographical Regions

The normalized regional monthly frequency is defined as the ratio of 20-year accumulated occurrence number in one month in each geographical region to the total grid number of each region. Fig. 3 illustrates the normalized monthly

Table 2 Summary of future change of occurrence ratio in each prefecture in the regions of Chugoku, Kyushu, Shikoku, Kinki and Chubu. The occurrence ratio (F1, F2, F3, F4, and F5) is defined as the ratio of total extracted events from one future climate dataset to the total events from the present climate dataset of SPA. The cells with decreasing trends are highlighted by the background color of grey.

Region	Prefecture	Grids	SPA	Future Climates†					
				F1	F2	F3	F4	F5	Fave
Chugoku	Yamaguchi	6330	2.7	1.1	1.5	2.4	2.8	1.7	2.1
	Hiroshima	8413	2.8	1.7	2.4	2.6	3.2	1.4	2.4
	Okayama	6925	3.5	1.2	1.6	1.4	1.4	0.8	1.3
	Shimane	6549	0.2	4.6	6.5	9.7	16.7	9.8	10.7
	Tottori	3409	1.7	2.5	3.3	2.6	2.4	1.1	2.3
Kyushu	Fukuoka	4909	2.3	0.6	1.9	2.1	2.0	1.7	1.9
	Kumamoto	7179	3.4	0.8	1.5	1.9	2.2	1.7	1.8
	Nagasaki	5019	3.1	1.1	1.5	2.4	2.2	2.0	2.0
	Oita	6161	4.3	1.1	1.5	1.7	1.6	1.3	1.5
	Kagoshima	9529	2.6	1.3	1.7	2.3	2.5	2.2	2.2
	Saga	2391	4.6	0.8	1.8	2.5	2.1	1.5	2.0
	Miyazaki	7275	1.5	2.5	2.2	4.0	3.2	2.8	3.0
	Okinawa	1641	1.6	1.5	1.9	3.7	3.5	2.1	2.8
Shikoku	Ehime	5883	5.7	1.8	1.6	2.3	1.9	1.5	1.8
	Kagawa	2045	3.2	0.9	1.1	1.4	0.3	0.5	0.8
	Kochi	6877	1.6	2.0	1.4	2.0	2.1	1.6	1.8
	Tokushima	4002	4.6	1.1	1.2	1.6	1.0	1.2	1.2
Kinki	Hyugo	8248	1.9	1.2	1.5	2.1	1.7	1.2	1.6
	Kyoto	4495	1.5	1.7	1.8	3.4	1.8	1.3	2.1
	Nara	3472	4.1	1.1	0.7	1.2	1.3	1.4	1.2
	Osaka	1878	0.7	2.1	0.8	3.0	2.0	1.8	1.9
	Shiga	3300	2.9	1.0	1.1	2.2	1.7	1.2	1.5
	Wakayama	4614	2.1	1.7	2.0	2.5	2.6	3.3	2.6
Chubu	Aichi	5102	1.5	1.1	1.8	3.0	3.7	1.8	2.6
	Mie	5733	4.8	1.0	1.1	1.6	1.5	1.5	1.4
	Fukui	4195	1.1	2.3	2.1	3.3	3.1	3.1	2.9
	Ishikawa	4334	1.1	1.9	2.3	3.0	2.2	2.6	2.5
	Gifu	10164	0.9	1.6	2.1	2.3	4.0	2.0	2.6
	Toyama	4168	0.8	1.4	3.4	2.3	2.3	2.4	2.6
	Yamanashi	4275	4.2	1.1	1.2	2.1	2.2	1.3	1.7
	Shizuoka	7592	6.4	1.2	1.5	2.1	2.7	1.5	2.0
	Niigata	12609	0.2	2.1	4.2	9.5	6.6	6.0	6.6
	Nagano	13027	3.9	1.0	1.6	2.1	2.5	1.7	2.0

†Definition: F1 = SFA_26 / SPA, F2 = SFA_c1 / SPA, F3 = SFA_c2 / SPA, F4 = SFA_c3 / SPA, F5 = SFA_c0 / SPA; Fave = (F2 + F3 + F4 + F5) / 4

frequency of the present and future climates in different geographical regions. In the Kyushu and Chugoku regions in west Japan, the estimated landslide occurrence is higher in July in the early summer. But, in the Tohoku and Kanto regions in east Japan, the estimated frequency is much higher in September in the late summer. Between east and west Japan, the estimated future landslide frequency

Table 3 Summary of future change of occurrence ratio in each prefecture in the regions of Kanto, Tohoku and Hokkaido. The occurrence ratio (F1, F2, F3, F4, and F5) is defined as the ratio of total extracted events from one future climate dataset to the total events from the present climate dataset of SPA. The cells with decreasing trends are highlighted by the background color of grey.

Region	Prefecture	Grids	SPA	Future Climates†					
				F1	F2	F3	F4	F5	Fave
Kanto	Ibaraki	5880	3.3	1.7	2.0	2.6	3.0	1.7	2.3
	Gunma	6146	2.4	1.3	1.9	2.1	3.1	2.2	2.3
	Tochigi	6196	3.1	1.1	1.1	2.3	2.5	1.4	1.8
	Saitama	3633	1.4	1.7	1.6	3.1	2.8	2.2	2.4
	Tokyo	2347	2.3	1.3	2.0	2.3	2.8	1.9	2.2
	Chiba	5154	5.3	0.6	1.5	1.5	1.2	1.2	1.4
	Kanagawa	2441	3.4	1.2	1.7	1.7	2.5	1.3	1.8
Tohoku	Fukushima	13473	3.8	1.4	1.3	1.7	2.6	1.3	1.7
	Miyagi	7484	3.8	1.1	1.6	2.2	3.5	1.9	2.3
	Yamagata	9307	0.8	2.1	4.4	4.9	6.4	3.6	4.8
	Iwate	15626	2.6	1.0	1.6	2.2	3.4	2.1	2.3
	Akita	11849	0.7	1.7	4.8	3.1	5.1	3.5	4.1
	Aomori	10225	0.5	2.6	6.0	4.1	8.0	4.1	5.5
Hokkaido	Rumoi §	3839	0.0	1.0	14.0	6.9	5.7	9.4	9.0
	Tokachi	11543	0.2	1.0	6.0	5.3	8.1	4.9	6.1
	Kushiro&Nemuro §	10343	0.0	2.8	10.6	11.2	38.4	10.0	17.5
	Ishikari&Sorachi	9923	0.2	0.8	2.1	2.3	4.3	4.7	3.3
	Shouya	5314	0.2	3.6	21.6	25.0	15.8	14.7	3.9
	Shiribeshi	4708	0.2	2.0	4.0	2.7	5.1	3.9	3.9
	Ohotsuku §	11517	0.0	122.2	378.5	161.0	479.7	220.4	309.9
	Oshima&Hiyama	7232	0.2	1.3	7.4	7.5	10.0	8.1	8.2
	Iburi&Hidaka	9123	0.2	0.7	3.5	3.8	5.5	4.7	4.4
	Kamikawa §	11420	0.0	∞	∞	∞	∞	∞	∞

† Definition: F1 = SFA_26 / SPA, F2 = SFA_c1 / SPA, F3 = SFA_c2 / SPA, F4 = SFA_c3 / SPA, F5 = SFA_c0 / SPA; Fave = (F2 + F3 + F4 + F5) / 4

§ Events in SPA: Rumoi = 177, Ohotsuku = 13, Shouya = 185, Kushiro&Nemuro = 390, Ohotsuku = 0

is higher in July, August, and September in the Chubu, Kinki, Shikoku, and Hokkaido regions. Particularly, in September the Tohoku region holds the highest estimated frequency of 3.4 from SFA_c3 which is 1.5 times higher than the ones from other datasets.

3.3 Risk Features in Each Prefecture

Tables 2 and 3 tabulate the future change of landslide risk in each prefecture. From SFA_26 and SFA_c0 representing El Niño, we can find slight decreases of occurrence in Fukuoka, Kumamoto, Saga, Okayama, Kagawa, Chiba, Ishikari, Sorachi, Iburi, and Hidaka as well as in Osaka and Nara from SFA_c1. Particularly, Kagawa holds the most decreasing trends from three datasets and the mean ratio of 0.8, as is listed in Table 2. The Tohoku and Hokkaido regions have the occurrence ratios which are all higher than two and the mean ratios of more than 3.0.

3.4 Landslide Risk in Tectonic Zones

Our analysis adopts six tectonic zones, including East Hokkaido, Northeast Japan, Fossa

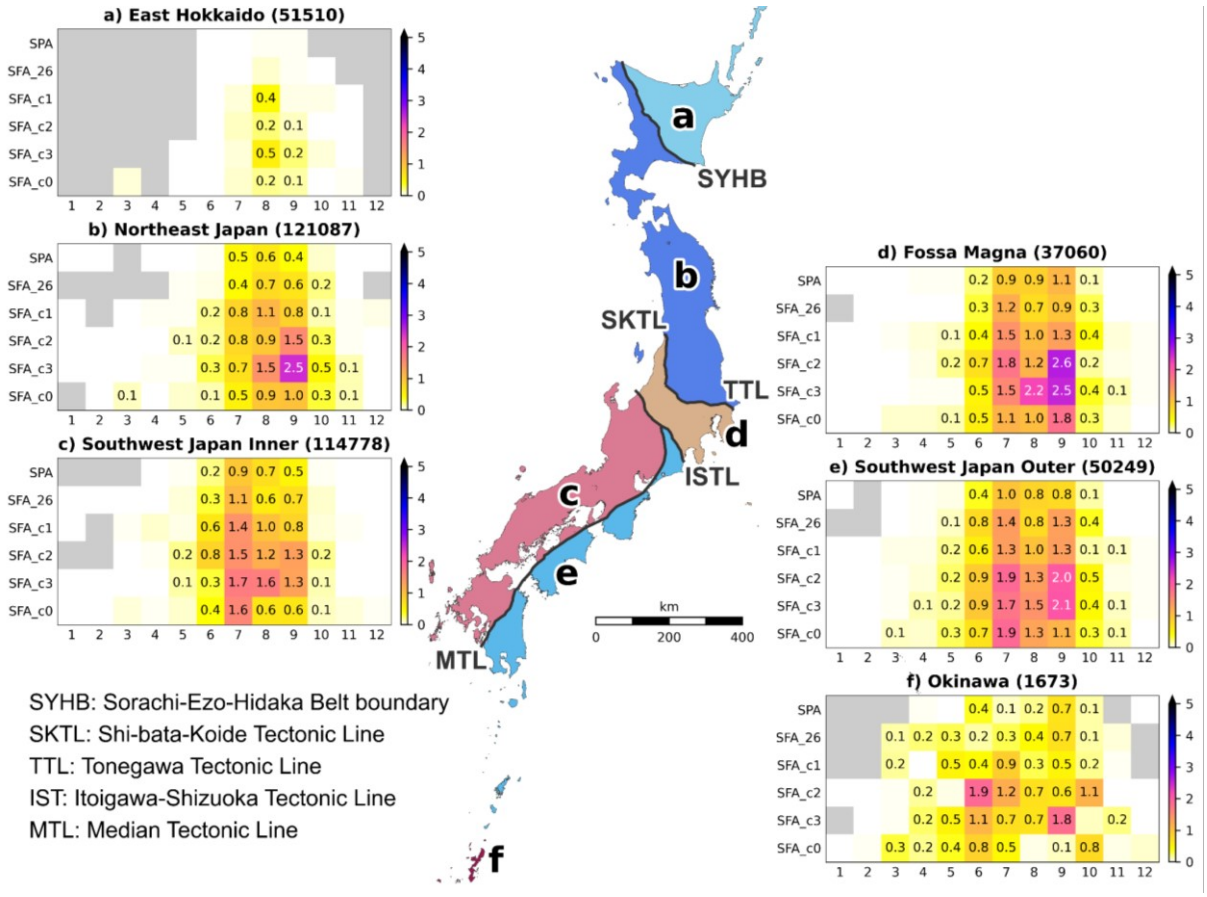

Fig. 4 Normalized monthly frequency from six NHRCM05 datasets in size tectonic zones of a) East Hokkaido, b) Northeast Japan, c) Southwest Japan inner belt, d) Fossa Magna, e) Southwest Japan outer belt, and f) Okinawa. The cell values and colors denote the normalized monthly frequency. Gray color denotes non-occurrence. The total grid numbers are denoted in brackets.

Magna, Southwest Japan Inner and Outer Belts, and Okinawa, as are shown in Fig. 4. Here we adopt Tonegawa Tectonic Line to separate the northeast and southeast Japan (Takahashi, 2006), and use the range between Hidaka and Sorachi-Ezo Belts as a plate boundary in central Hokkaido (Takahashi, 2016). Regarding the bedrock composition, the Paleogene or older rocks are widely exposed to the Earth's surface in Southwest Japan Arc, whereas the Neogen or Quaternary sediments cover large areas of the Northeast Japan (Takahashi, 2016). Thus, these characteristics of tectonic zones may exert explicit influences to landslide risk (MLIT, 2020). As a result, under rainy weathers varying from zone to zone in a changing climate, each tectonic zone possessing different bedrocks exhibits specific situations of landslide risk, as mentioned below. The Southwest Japan Inner Belt is just located at a hot zone of Baiu fronts and holds higher corresponding landslide risk in the early summer. Then, the zones of East Hokkaido and Northeast Japan in higher latitudes have higher landslide risk in the late summer, probably due to the higher potential of typhoon strikes. On the other hand, the zones of Fossa Magna, Southwest Japan Outer Belt, and Okinawa would be impacted both by Baiu fronts and typhoons, so the landslide risk in these zones appears fairly equivalent between July and September. Particularly, the Okinawa zone has a longer period from Spring to Fall to hold fair high landslide risk.

4. Conclusions

Through the application of the critical line method to NHRCM05, we exhibit the future changes of landslide risk in the whole Japan in

terms of the estimated total and monthly frequency on the nationwide scale and in the geographical regions, individual prefecture, and six tectonic zones. In summary, landslide risk would definitely be risen up between July and September in the future, but only Kagawa would face a future decreasing trend. The period between July to September could match the present climate in Japan that the Baiu season comes in June and July, and the typhoon season follows between August and October. If the sea-surface temperature around Japan is higher, the landslide hot zones are along the coast of Pacific Ocean in the Kanto and Tohoku regions in September. This would probably be due to the increase of projected cyclone precipitation even though the cyclone number decreases in the future projections of NHRCM05 (Watanabe et al., 2019). Also, the high landslide risk in west Japan in July would attribute to more frequent heavy rainfall in the Baiu season in the NHRCM05 future projections (Osakada and Nakakita, 2018). Moreover, the tectonic zones of East Hokkaido and Northeast Japan would hold a higher risk of landslides triggered by typhoons in the late future summer, and the other zones would face landslides both by Baiu fronts and typhoons between June to October.

So far, through this research, we have successfully demonstrated the spatiotemporal characteristics of landslide risk. The relation between rainfall types and landslide risk is still unclear. The number of climate simulation used for analysis is also too few to obtain the statistical characteristics. So, with more climate simulation datasets, our future work will aim at further examining this relation to the influence of types of rainfall on the future change of landslide risk.

Acknowledgements

This work was supported by the Integrated Research Program for Advancing Climate Models (TOUGOU) Grant Number JPMXD0717935498 from the Ministry of Education, Culture, Sports, Science and Technology (MEXT), Japan. The authors appreciate the courtesy of MLIT Sabo Planning Division, JMA, and all Prefectural Governments for sharing the data of all critical lines. The tectonic zones were derived from 200,000:1 Seamless Geological Map of Japan V2 published by Geological Survey of Japan.

References

Kawagoe, S., Kazama, S. and Sarukkalige, P. (2010): Probabilistic modelling of rainfall induced landslide hazard assessment, Hydrol. Earth Syst. Sci., Vol. 14, pp.1047-1061.

MLIT (2005): Manual of Determining Rainfall Threshold for Early-Warning of Sediment Disasters.

MLIT (2020): Committee Discussions on Technology and Evaulation of Sediment Disasters under Climate Change.

Murata, A., Sasaki, H., Kawase, H., Nosaka, M., Oh'izumi, M., Kato, T., Aoyagi, T., Shido, F., Hibino, K., Kanada, S., Suzuki-Parker, A. and Nagatomo, T. (2015): Projection of future climate change over Japan in Ensemble Simulations with a High-Resolution Regional Climate Model, SOLA, Vol. 11, pp. 90-94.

Murata, R., Arakawa, O., Ose, T., Kusunoki, S., Endo, H. and Kitoh, A. (2014): Classification of CMIP5 Future Climate Responses by the Tropical Sea Surface Temperature Changes, SOLA, Vol. 10, pp. 167-171.

Osakada, Y. and Nakakita, E. (2018): Future Change of Occurrence Frequency of Baiu Heavy Rainfall and Its Linked Atmospheric Patterns by Multiscale Analysis, SOLA, Vol. 14, pp. 79-85.

Osanai, N., Shimizu, T., Kuramoto, K., Kojima, S. and Noro, T. (2010): Japanese early-warning for debris flows and slope failures using rainfall indices with Radial Basis Function Network, Landslides, Vol. 7, pp. 325-338.

Saito, H., Korup, O., Uchida, T., Hayashi, S. and Oguchi, T. (2014): Rainfall conditions, typhoon frequency, and contemporary landslide erosion in Japan, Geology, Vol. 42, No. 11, pp. 999-1002.

Sasaki, H., Murata, A., Hanafusa, M., Oh'izumi, M. and Kurihara, K. (2011): Reproducibility of Present Climate in a Non-Hydrostatic Regional Climate Model, SOLA, Vol. 7, pp. 173-176.

Sasaki, H., Murata, A., Hanafusa, M., Oh'izumi, M.

and Kurihara, K. (2012): Projection of Future Climate Change in a Non-Hydrostatic Regional Climate Model Nested within an Atmospheric General Circulation Model, SOLA, Vol. 8, pp. 53-56.

Takahashi, M. (2016): Geological problem for the tectonic boundary between Northeast and Southeast Japan. -The beginning-, GSJ CHISHITSU NEWS, Vol. 5, No. 7, pp. 218-225.

Takahashi, M. (2006): Tectonic boundary between Northeast and Southwest Japan Arcs during Japan Sea opening, Jour. Geol. Soc. Japan, Vol. 112, No. 1, pp. 14-32.

Watanabe, S.I., Murata, A., Sasaki, H., Kawase, H. and Nosaka, M. (2019): Future Projection of Tropical Cyclone Precipitation over Japan with a High-Resolution Regional Climate Model, J. Meteorol. Soc. Jpn., Vol. 97, No. 4, pp. 805-820.

(Received August 31, 2020)